Nanostructured CNx (0 <x <0.2) films grown by supersonic cluster beam deposition

Bongiorno, G; Blomqvist, M; Piseri, P; Milani, P; Lenardi, C; Ducati, C; Caruso, T; Rudolf, P; Wachtmeister, S; Csillag, S

Published in:
Carbon

DOI:
10.1016/j.carbon.2005.01.022

Available online at www.sciencedirect.com
SCIENCE DIRECT®
Carbon 43 (2005) 1460–1469
CARBON
www.elsevier.com/locate/carbon

Nanostructured CN_x ($0 < x < 0.2$) films grown by supersonic cluster beam deposition

G. Bongiorno [a,b], M. Blomqvist [a], P. Piseri [a,b], P. Milani [a,b,*], C. Lenardi [c,b], C. Ducati [d], T. Caruso [e], P. Rudolf [f], S. Wachtmeister [g], S. Csillag [g], E. Coronel [h]

[a] INFM-Dipartimento di Fisica, Università di Milano, Via Celoria 16, I-20133 Milano, Italy
[b] Centro Interdisciplinare Materiali ed Interfacce Nanostrutturati (CIMAINA), Universitá di Milano, Via Celoria 16, I-20133 Milano, Italy
[c] INFM-Istituto di Fisiologia Generale e Chimica Biologica, Universitá di Milano, Via Trentacoste 2, 20134 Milano, Italy
[d] Department of Material Science and Metallurgy, University of Cambridge, Pembroke street CB2 3QZ, Cambridge, United Kingdom
[e] INFM-Dipartimento di Fisica, Universita' della Calabria, Ponte Bucci, I-87036 Arcavacata di Rende (CS), Italy
[f] Materials Science Centre, Rijksuniversiteit of Groningen, Nijenborgh 4 9747 AG Groningen, The Netherlands
[g] Department of Physics, Stockholm University, SCFAB, SE-106 91 Stockholm, Sweden
[h] Department of Materials Science, The Ångström Laboratory, Uppsala University, Box 534, 75121 Uppsala, Sweden

Received 22 October 2004; accepted 22 January 2005
Available online 2 March 2005

Abstract

Nanostructured CN_x thin films were prepared by supersonic cluster beam deposition (SCBD) and systematically characterized by transmission electron microscopy (TEM), electron energy-loss spectroscopy (EELS), X-ray photoelectron spectroscopy (XPS) and scanning electron microscopy (SEM). The incorporation of nitrogen in the films ($0 < x < 0.2$) and the nanostructure were controlled by using different synthesis routes. Films containing bundles of well-ordered graphene multilayers, onions and nanotubes embedded in an amorphous matrix were grown alongside purely amorphous films by changing the deposition parameters. Graphitic nanostructures were synthesized without using metallic catalysts. The structural and electronic properties of the films have been studied by EELS. The role played by N in the carbon nanostructures has been deduced from XPS line-shape analysis.

Keywords: C. Electron energy loss spectroscopy, Electron microscopy, X-ray photoelectron spectroscopy; D. Electronic structure, Chemical structure

1. Introduction

Following the theoretical prediction of the existence of superhard β-C_3N_4 structure [1] and the discovery of carbon fullerenes [2], carbon nanotubes [3] and of their novel mechanical properties, great efforts have been devoted to the synthesis of nanostructured CN_x thin films [4–6]. Fullerene-like materials composed of CN_x graphene multilayers, onions and nanotubes together with amorphous structures have been already synthesized by different deposition techniques, e.g. unbalanced reactive magnetron sputtering [4], anodic jet carbon arc [5], DC arc evaporation [6]. It has been demonstrated that the physical properties of these materials, like for example hardness and elasticity, can be modified to a very large extent by changing both the structure at the nanometer scale and the nitrogen content [4].

In this work we report on the synthesis of CN_x thin films by supersonic cluster beam deposition by which CN_x nanosized building blocks are directly deposited on the substrate without substantial fragmentation at

* Corresponding author. Tel.: +39 02 503 17350; fax: +39 02 503 17482.
E-mail address: pmilani@mi.infn.it (P. Milani).

0008-6223/$ - see front matter © 2005 Elsevier Ltd. All rights reserved.
doi:10.1016/j.carbon.2005.01.022

the impact. By means of EELS, XPS, TEM and SEM, we demonstrate that it is possible to modify the nitrogen content, the morphology and the electronic structure of the CN_x films by changing the cluster formation and deposition conditions. A big advantage of SCBD is that films can be deposited on any kind of substrate and that the deposition is done at room temperature. Moreover the high directionality achievable by supersonic beams can be exploited to realize patterned depositions with stencil masks (this makes SCBD compatible with the other planar microtechnologies [7]).

2. Experimental

Nanostructured CN_x films have been grown in a deposition apparatus equipped with a pulsed microplasma cluster source (PMCS) and a filamentless ion beam source mounted as shown in Fig. 1.

The operation principle of a PMCS has been described elsewhere [8]. Briefly, the source consists of a ceramic body with a channel drilled to intersect perpendicularly a larger cylindrical cavity (Fig. 1). The channel hosts two graphite rods (purity 99.999%) separated by a gap. A solenoid pulsed-valve faces one side of the cavity. A removable nozzle closes the other side of the cavity. The solenoid valve, backed with a pressure of 20 bar, delivers He pulses with an opening time of few hundreds of microseconds and a repetition rate between 1 Hz and 10 Hz. An intense helium jet is formed towards the cathode surface facing the valve, producing a suitable pressure for plasma generation [8]. During standard operation the mean He pressure in the source cavity is of roughly 1 Torr. Before the valve closes, a voltage ranging from 500 V up to 1500 V is applied to the rods, causing the ignition of the discharge and the production of the plasma. The ablation occurs when helium plasma strikes the cathode surface removing atoms via sputtering.

The sputtered carbon atoms thermalize with the buffer gas and condense to form clusters. The gas–cluster mixture is then expanded through the source nozzle into an expansion chamber to form a supersonic beam [8]. The supersonic cluster beam enters the deposition chamber passing through a skimmer and it is intercepted by the substrate.

With typical PMCS operation conditions, one obtains a lognormal cluster mass distribution in a range from few tenths to several thousands of atoms per cluster, with an average size at about 1000 atoms/cluster [9]. The kinetic energy of the clusters is lower than 0.4 eV/atom, well below the binding energy of carbon atoms in the clusters. At cluster impact on the surface there is thus no substantial fragmentation of the aggregates and deposited films keep memory of the structure the clusters had in the gas phase [10].

In the present experiments the source nozzle was an aerodynamical focusing assembly consisting of a sequence of drilled thin plates, the aerodynamic lenses [11,12], mounted at the end of cylindrical spacers, called focusing modules. The final module is designed as a sonic lens nozzle [13]. This configuration allows the focalization of the clusters on the axis of the beam [11–13]. Moreover, this system permits to aerodynami-

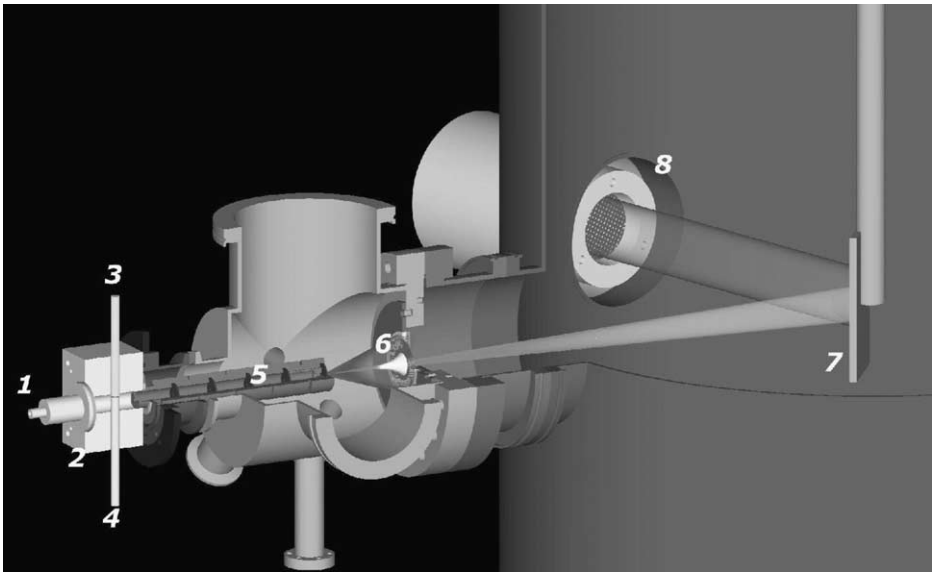

Fig. 1. Schematic representation of a vertical section of the deposition apparatus. On the left side one can see the PMCS operating outside the vacuum. A pulsed valve (1) and two electrodes (3) and (4) are mounted on the ceramic body (2). The aerodynamic focusing nozzle with five lenses (5) is protruding in the evacuation chamber which is separated by the deposition chamber by a skimmer (6). A substrate mounted on the sample holder (7) can collect the supersonic cluster beam exiting the skimmer and the ion beam produced by the ion gun source (8).

cally select the size of the clusters depending on its geometry and on the carrier gas used [11–13].

The cluster beam intensity has been characterized in the deposition chamber by a quartz microbalance positioned at a distance of 500 mm from the source nozzle and of 20 mm from the sample manipulator. The microbalance measures the beam intensity in terms of deposition rate on its active surface of 47.7 mm^2. With a discharge voltage of 750 V at 1 Hz of repetition rate, deposition rates of 25 nm/min are obtained using the aerodynamical focusing nozzle.

The filament-less ion gun source, an Ion-Tech RF/F40 placed on an ISO 160 KF mounting flange, is operated with a 13.56 MHz RF power supply and generates a collimated ion beam with a diameter of 4 cm. We operated the source with nitrogen. A flat Faraday probe was used to measure the average ion flux produced by the ion gun source at the substrate position. The flux of nitrogen ions accelerated at a kinetic energy of 100 eV and 300 eV was in the range of hundreds of $\mu A/cm^2$.

The PMCS source and the ion gun source are mounted on a high vacuum deposition apparatus (Fig. 1). The PMCS is connected by means of a KF 40 flange to an expansion chamber, which is independently pumped and separated from the deposition chamber through an electroformed skimmer. The filament-less ion gun source is directly mounted on the deposition chamber at an angle of 75° between the deposition axis of PMCS and the ion gun source. The pumping system of the PMCS expansion chamber (2.5 dm^3) is composed of a Roots pump (270 m^3/h) backed by a rotary pump (120 m^3/h); the background pressure achieved is in the 10^{-3} Torr range while during source operation the mean pressure is of 10^{-1} Torr. The deposition chamber (200 dm^3) is evacuated by means of a turbomolecular pump (1000 l/s) backed by a Scroll pump (600 l/min), yielding a background pressure in the low 10^{-6} Torr range which increases to 5×10^{-4} Torr during film deposition because of the gas injected through both PMCS and ion gun source. The sample holder is placed in the deposition chamber on an automated four-axis manipulator (x–y–z and a rotation θ) remotely controlled with a personal computer.

Different deposition protocols have been used in order to investigate the role of nitrogen incorporation on the film nanostructure. A group of films have been grown by operating the PMCS with two different nitrogen-containing gasses instead of pure He: N_2 and a mixture of He (81%) and NH_3 (19%). In this way nitrogen is available and it can be incorporated during the cluster formation. A second group of films have been produced by the deposition of carbon clusters assisted by a nitrogen ion flux at different kinetic energies (100 eV and 300 eV). In the following we shall refer to these samples as ns-C, N_2 gas synthesized CN_x, NH_3 gas synthesized CN_x, 100 eV or 300 eV N^+ assisted ns-C, respectively. All the samples have been grown at room temperature since SCBD does not induce any substrate heating [7].

Films were grown on Si substrates for scanning electron microscopy (SEM) and X-ray photoelectron spectroscopy (XPS) analysis; before the deposition these substrates were ultrasonically cleaned in acetone. For transmission electron microscopy (TEM) and electron energy loss spectroscopy (EELS) characterization films were grown on freshly cleaved NaCl substrates, floated off from the NaCl substrates in distilled water and picked up on a holey carbon TEM grid. All the samples were exposed to air after deposition.

TEM characterization has been performed with a Philips/Tecnai microscope (field emission gun operated at 300 keV) and with a Jeol FX3010 microscope (LaB_6 filament electron gun operated at 300 keV). EELS measurements were carried out with the Philips/Tecnai TEM microscope. EELS was performed in parallel to TEM imaging with a diameter of the electron beam at the sample of 35 nm and an energy resolution of 1.4 eV. SEM characterization was done with a Jeol JSM-6400F field emission scanning electron microscope operated with an accelerating voltage of 30 kV.

The XPS spectra were collected using a SSX-100 (Surface Science Instruments) photoelectron spectrometer with a monochromatic Al Kα X-ray source ($h\nu$ = 1486.6 eV). The energy resolution was set to 0.7 eV and the photoelectron take-off angle (TOA) was 54°. The beam diameter of the monochromatized Al Kα source was 150 μm, and a hemispherical electron energy analyzer with a multichannel detection system was used. Spectral analysis included a Shirley background subtraction and peak separation using Gaussian functions, in least squares curve-fitting program (Winspec) developed in the LISE laboratory of the Facultés Universitaires Notre-Dame de la Paix, Namur, Belgium.

3. Results and discussion

3.1. Chemical composition

XPS was employed to quantify the chemical composition of the surface of our samples and to identify contaminants. As reported in Table 1, XPS wide spectra (0–1000 eV in binding energy) gave evidence for the presence of C, N and O and no other chemical elements could be detected in any of the samples.

Oxygen and nitrogen contents seem to be independent from each other. The oxygen percentage, calculated with respect to C content, ranges from 10% to 21% and does not appear to be linked to deposition conditions. On the contrary, the nitrogen concentration, also referred to C content, ranges from 2% to 20% and depends on the deposition process. The lowest N content (2%) is found in pure ns-C.

Table 1
Chemical composition of the prepared samples measured by XPS. The atomic percentages of O and N referred to C content are reported in brackets (O/C and N/C)

	C (at.%)	O (at.%)	N (at.%)
ns-C	86.4	11.9 (13.8)	1.7 (2.0)
N_2 gas synthesized CN_x	82.4	8.7 (10.6)	8.9 (10.8)
NH_3 gas synthesized CN_x	79.1	15.0 (19.0)	5.9 (7.5)
100 eV N^+ assisted ns-C	70.8	15.1 (21.3)	14.1 (19.9)
300 eV N^+ assisted ns-C	74.0	14.0 (18.9)	12.0 (16.2)

3.2. Nanostructure

In Fig. 2 we show, as a reference, a TEM image of a pure ns-C film produced without N doping. The film consists of a random assembly of highly curved graphene sheets interlinked and aggregated to form a disordered and irregular nanostructure.

The nanostructure of a film grown with clusters obtained with N_2 as buffer gas instead of He is reported in Fig. 3. This film contains better developed graphene sheets which are closely packed. The average curvature radius of the sheets is larger than for the ns-C sample. Onion-like particles consisting of few shells are also visible. The nitrogen incorporation in carbon clusters appears to favor the formation of relatively large curled graphitic structures.

The nanostructure of CN_x films obtained by mixing NH_3 and He is shown in Fig. 4a–c and characterized by the coexistence of interwoven graphitic planes, onion-like nanoparticles and multi-walled nanotubes embedded in an amorphous matrix. The structures reported in Fig. 4a and b have a typical interlayer distance of graphene planes in MWNT (0.35 nm as reported in [14]). The structure reported in Fig. 4c is very similar to those observed by the groups of Amaratunga [5,15] and Hultman [4,16]. The films produced by means of anodic jet carbon arc driven by a N_2 gas jet [15] were found to contain aligned multi-walled carbon nanotubes

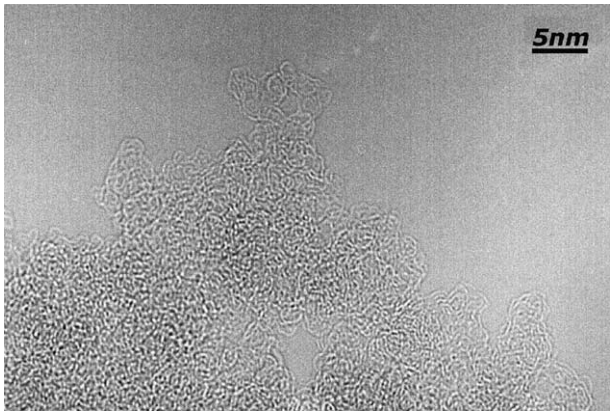

Fig. 2. TEM micrograph of a ns-C film. It is grown by collecting the carbon clusters produced operating the PMCS with He.

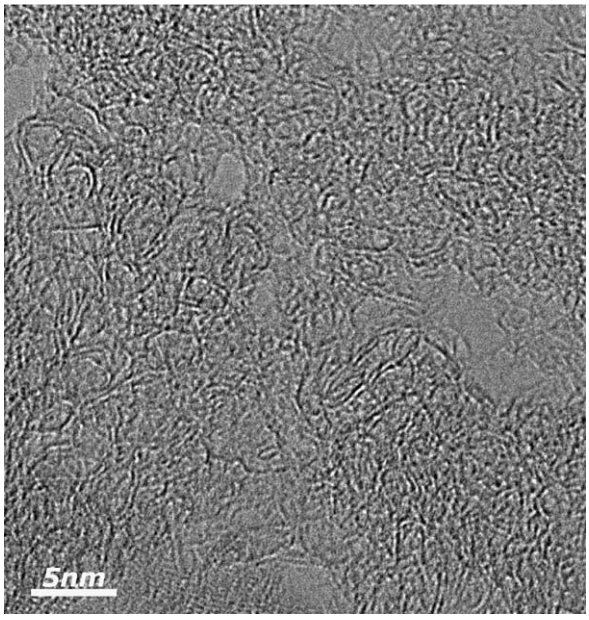

Fig. 3. TEM micrograph of N_2 gas synthesized ns-C film. N_2 is used instead of He in the PMCS for cluster production and expansion to form a supersonic beam.

and fullerene-like nanoparticles embedded in an amorphous carbon matrix [15]. Hultman et al. deposited fullerene like CN_x films by means of dual dc unbalanced reactive magnetron sputtering using a pure pyrolytic graphite target in a mixed Ar/N_2 discharge. The material consists of bent and intersecting graphitic basal planes with an interplanar lattice spacing of 0.35 nm. The degree of curvature, extent and alignment of the sheets depend on the operative condition of the deposition [16].

The effect of N ion assisted cluster deposition on the nanostructure of the CN_x films is shown in Fig. 5. For a 100 eV N^+ assisted ns-C thin film (Fig. 5) we observe the formation of irregular curved graphene planes with curvature radii in the 0.5–2 nm range. Overall the film results from an overlap of curved fragments. Comparing this microstructure with the ns-C film, we can say that, as in the case of N_2 gas synthesized CN_x, nitrogen incorporation seems to increase the number and the dimensions of ordered sp^2 structures in the film.

Increasing the N ions energy to 300 eV the structure at the nanoscale becomes amorphous. This can be attributed to the fact that carbon clusters deposited on the substrate are damaged by the impinging higher-energy ions [17].

In Fig. 6a we present the structure of a NH_3 gas synthesized CN_x film at a micrometer scale: it is porous with grains of a 100–200 nm diameter, and some grains are aggregated into larger islands. The 300 eV N^+ assisted ns-C thin film SEM image, shown in Fig. 6b, displays a rough surface with irregular and sharp grains of a diameter of 50–100 nm. Comparing the SEM images of the films, the 300 eV N^+ assisted ns-C thin film has a rougher

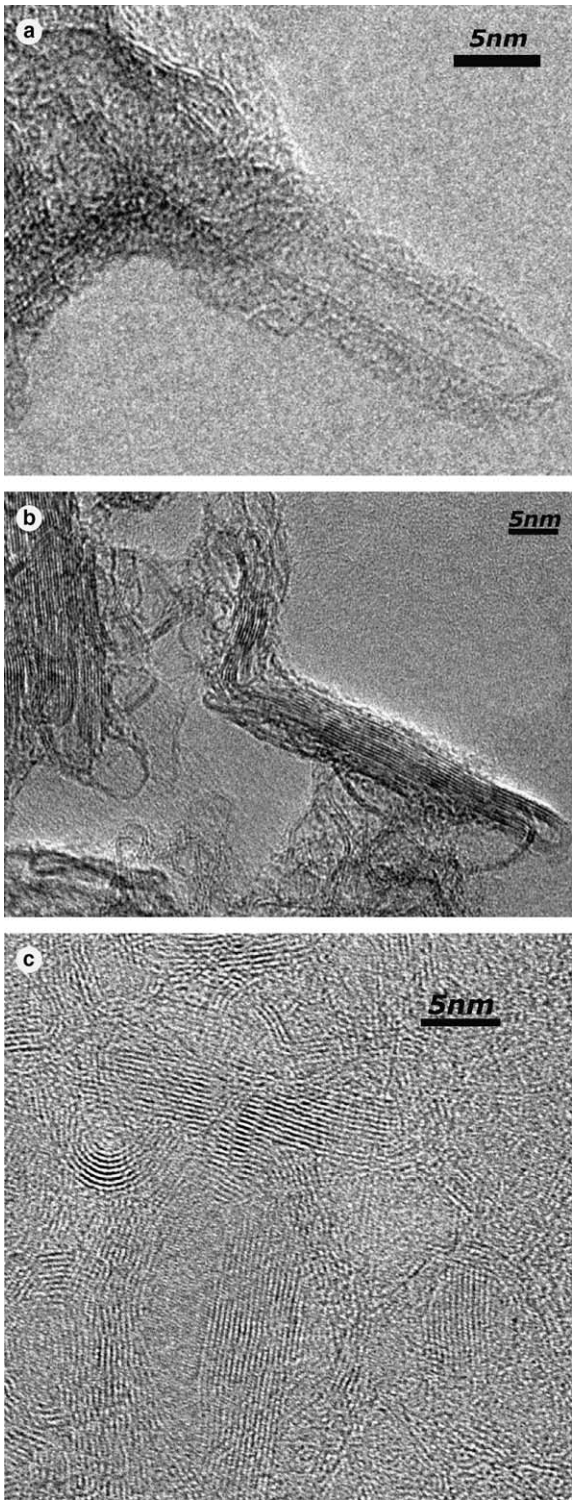

Fig. 4. TEM micrographs of NH_3 gas synthesized ns-C film. This material is obtained operating the PMCS with a mixture of He (81%) and NH_3 (19%). (a) A double-wall nanotube; (b) curled graphitic layers and nanoparticles; (c) densely packed graphitic planes and onion-like particles.

surface than the 100 eV N^+ assisted ns-C thin film (see Fig. 6c). In fact, the SEM image reported in Fig. 6c demonstrates a smooth surface with an undulating pattern.

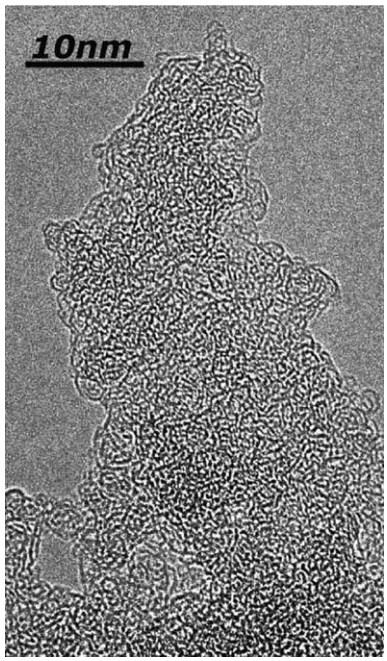

Fig. 5. TEM micrograph of a nanostructured film obtained by assisted deposition of carbon clusters with a 100 eV N^+ beam.

3.3. Electronic structure

We have used EELS and TEM analysis to investigate and correlate the electronic and the structural properties of different films. Thanks to the small irradiated sample area (diameter of 35 nm) EELS analysis has been performed in parallel to TEM imaging: the EEL spectra shown in Fig. 7 contain local information that correspond to the TEM micrographs described in the previous paragraph.

In the low-energy-loss region the EEL spectra of the different films are quite similar to amorphous carbon (a-C) spectra [18–20]. For all the different films the $\pi + \sigma$ plasmon peak occurs at 21–24 eV and has a very broad shape like in a-C [21]. The position of the $\pi + \sigma$ plasmon peak can vary from 23 eV for a-C to 26–27 eV for graphite and increases to 33 eV for diamond were only σ electrons are present [18,22]. The $\pi + \sigma$ plasmon peak in our films has a position that changes from 21 eV in the case of 300 eV N^+ assisted ns-C to 24 eV for NH_3 gas synthesized CN_x. This agrees with TEM images: the higher the degree of crystallization of the graphitic structures, the more the $\pi + \sigma$ peak position is similar to that of graphite.

Additional structural and electronic information can be obtained from the high-energy-loss region of the EEL spectra reported in Fig. 7. We measured the electron energy loss near the K-edges of C and N [23,24]. From core-loss peaks (C and N K-edge), which reflect the density of unoccupied states above the Fermi level in the presence of a core hole, we obtain information on the hybridization state of C and N [23–25].

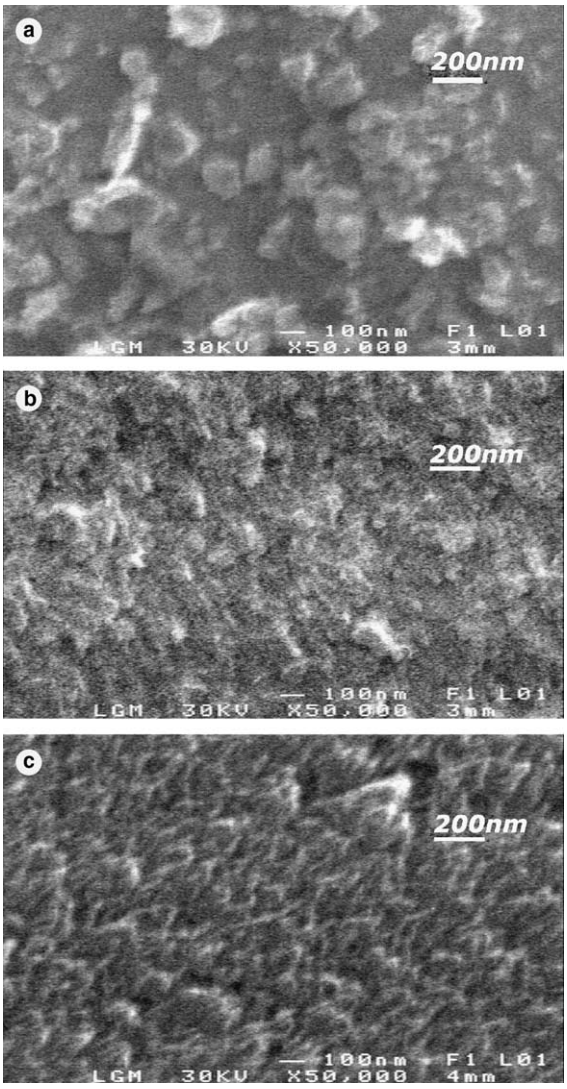

Fig. 6. SEM micrographs of the surfaces of: (a) NH_3 gas synthesized CN_x, (b) 300 eV N^+ assisted ns-C, (c) 100 eV N^+ assisted ns-C.

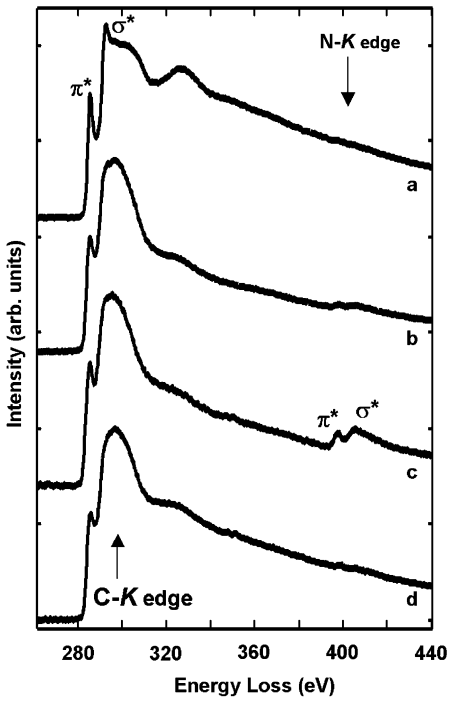

Fig. 7. C-K and N-K edges EELS spectra: (a) NH_3 gas synthesized ns-C, (b) N_2 gas synthesized ns-C, (c) 300 eV N^+ assisted ns-C, (d) ns-C. The position of π* and σ* peaks are indicated by an arrow for both C—K edge and N—K edge. Calcium signal at about 350 eV is visible in (c) and (d). This contamination is due to the preparation protocol used for TEM-EELS analysis.

The C K-edge has a characteristic shape that depends on the π- and σ-bonds configuration. The π* and σ* peaks correspond to the electron transitions from the C 1s core level to antibonding π* and σ* states, respectively. The intensity of the π*- and σ*-peaks mirrors the relative amount of π- and σ-bonding [15] and the shape of the σ*-peaks can give further details about the curvature of the nanostructures present in the films [23].

A smooth and broad σ peak and a distinct π* peak are the main features of the C K-edge of ns-C films, N_2 gas synthesized CN_x and 300 eV N^+ assisted ns-C. The shape of these spectra resembles that of the a-C [15,26,18]. Comparing the spectrum of ns-C with those of N_2 gas synthesized CN_x, NH_3 gas synthesized CN_x and 300 eV N^+ assisted ns-C, we can notice that the nitrogen addition seems to lead to an increase in the intensity of the π* peak. This is an indication that the π-bonding is increased. However there is no evidence of a correlation between the nitrogen contents measured by XPS and the π* peak intensity (see below). The NH_3 gas synthesized CN_x displays the highest σ* peak intensity; moreover, the complex structure of its σ* peak, similar to that of multi-walled nanotubes [23] and graphite [18], suggests a high degree of graphitic order. The results of this C K-edge analysis agree with the previous TEM observations.

The N K-edge intensity scales with N content and it is therefore not surprising that K-edge features become visible and well defined for N_2 gas synthesized CN_x and 300 eV N^+ assisted ns-C. As for the C K-edge, two components can be distinguished: the component at lower energy-loss corresponds to the N 1s-π* electron transition while the broad peak at higher energies represents the N 1s-σ* transition. The existence of the π* N K-edge peak signals the presence of π-bonded nitrogen in the films [24,25].

3.4. XPS line shape analysis

With XPS we have also studied the shapes of the C 1s, O 1s and N 1s photoemission lines of different films, which are shown in Figs. 8–10 respectively. The C 1s peak is broad and asymmetric indicating the presence of different components (Fig. 8). The main component,

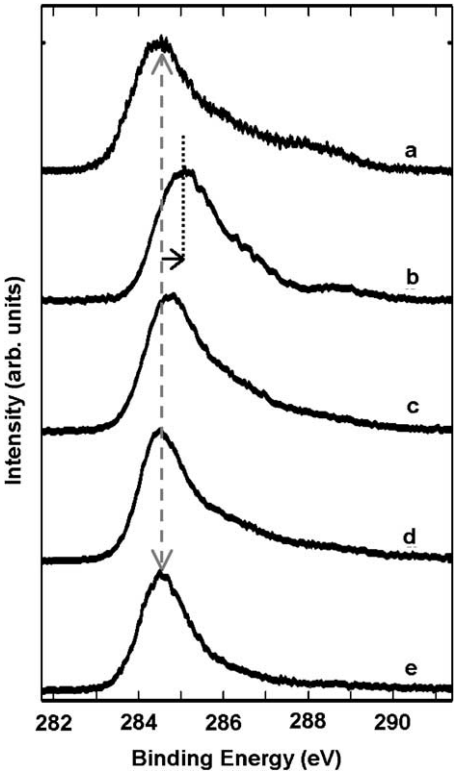

Fig. 8. XPS C 1s core-level spectra after background removal and normalization: (a) 100 eV N^+ assisted ns-C, (b) NH_3 gas synthesized ns-C, (c) 300 eV N^+ assisted ns-C, (d) N_2 gas synthesized ns-C, (e) ns-C.

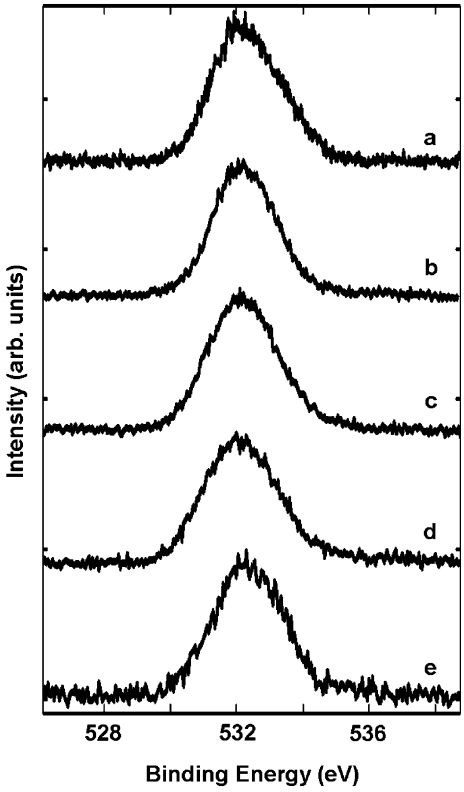

Fig. 9. XPS O 1s core-level spectra after background removal and normalization: (a) 100 eV N^+ assisted ns-C, (b) NH_3 gas synthesized ns-C, (c) 300 eV N^+ assisted ns-C, (d) N_2 gas synthesized ns-C, (e) ns-C.

unanimously attributed in literature to the C—C bonds in graphite [27], occurs at a binding energy 284.4–284.6 eV for all the films except the NH_3 gas synthesized CN_x. For the latter, it is found at 285 eV. This 0.5 eV shift for the NH_3 gas synthesized CN_x can be attributed either to hydrogen presence in the film [28,29] or simply to the nitrogen content in the film since electronegative groups will create an electron poor environment and push the C signal to higher binding energy[1] [30].

The other components needed to mathematically reconstruct the C 1s spectra are placed at higher binding energies and correspond to carbon directly bound to oxygen or nitrogen. Their chemical shift cannot be unambiguously attributed because of the contemporaneous presence of O and N in the films. Conflicting attributions can be found in literature: position and behavior of peaks change depending on the characteristics of the system studied [31] and usually the attribution considers either O or N even if both are present in the material [32,33]. However, since ns-C has a less structured C 1s peak and the O 1s photoemission line shape (see below) does not substantially change between the differently produced materials, we can say that the higher intensity of the high-energy component of the C 1s peak of N containing films is probably due to the formation of bonds between carbon and nitrogen.

The O 1s photoemission line is observed at about 532.1 eV binding energy (Fig. 9) and its FWHM is the same for the differently produced material (we observe a random shift of the oxygen peak of roughly 0.1 eV for different samples). This suggests that the nature of oxygen chemical bonding is the same in all of our films.

Also the N 1s photoemission line is observed at the same binding energy position for all of the films produced (Fig. 10). All spectra show a main double Gaussian peak structure suggesting that N is bonded essentially in two different bonding configurations. The binding energies found for the two peaks are 398.8 eV and 400.2 eV. An additional small component was introduced at 402 eV but its intensity is almost negligible.

In literature the N 1s photoemission line of carbonaceous systems with O and N containing groups is usually mathematically reconstructed with four peaks [34,16]: a first peak at 398 eV assigned to nitrogen bond to sp^3-hybridized carbon, a second one placed at 399.0 eV and assigned to pyridine-like nitrogen (N bonded to

[1] C.D. Wagner, A.V. Naumkin, A. Kraut-Vass, J.W. Allison, C.J. Powell, J.R. Rumble Jr., NIST X-ray photoelectron spectroscopy database 20, Version 3.4, Standard reference data program of the National Institute of Standards and Technology, USA, 2003.

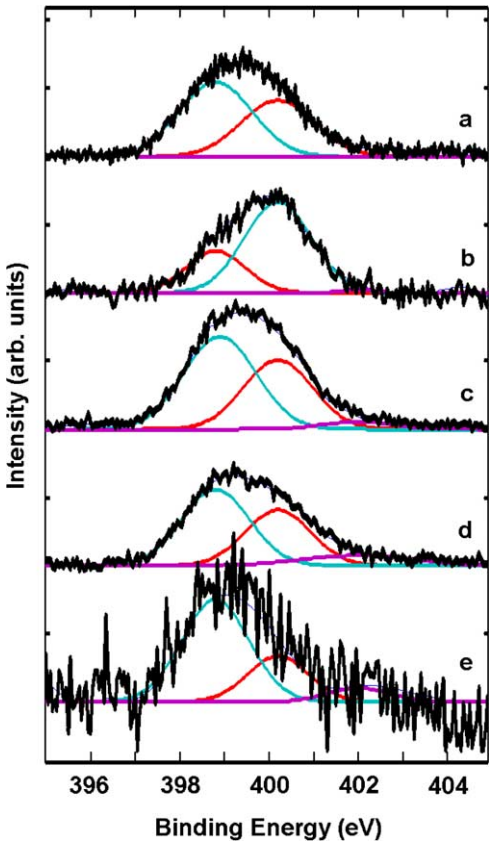

Fig. 10. XPS N 1s core-level spectra: (a) 100 eV N^+ assisted ns-C, (b) NH_3 gas synthesized ns-C, (c) 300 eV N^+ assisted ns-C, (d) N_2 gas synthesized ns-C, (e) ns-C. After background removal and normalization the spectra have been fitted by means of three Gaussian-shape peaks at 398.8 eV, 400.2 eV and 402 eV.

two sp^2-coordinated C atoms at the edge of a graphite sheet), a third one at 400.1 eV and corresponding to nitrogen bonded to three sp^2-coordinated carbon (substitutional nitrogen in a graphite sheet), and finally a fourth peak at 402 eV which is generally attributed to N—O bonds.

In the N 1s spectra of our films the peak at 398 eV (N bonded to sp^3 carbon) is completely absent. This agrees with the results obtained from EELS and TEM: our materials are prevalently constituted of sp^2 hybridized carbon.

The peak at 402 eV (N—O) is so weak that we can conclude that nitrogen and oxygen do not combine with each other but create separate bonds with carbon [34].

The presence of the peaks at 398.8 eV and 400.2 eV suggests that our materials are prevalently composed of graphene-like structures with nitrogen atoms as substitutional inclusions. It is reasonable to suppose that these nitrogen atoms can be found in the middle of a graphene plane bonded to three C atoms (giving rise to the peak at 400.2 eV [34]) or at the border of a graphene plane (creating in this case the pyridine-type peak at 398.8 eV [34]). Looking at the spectra of Fig. 10, the peak at 398.8 eV is always more intense than that at 400.2 eV except for NH_3 gas synthesized CN_x. This observation fits with the description of the samples given up to now: the nanostructure of NH_3 gas synthesized CN_x is prevalently composed of curved "longer" range-ordered graphene planes (small perimeter to area ratio);therefore there will be more nitrogen substitutional atoms located in the middle of these planes than N located at the borders (high intensity of the peak at 400.2 eV). Hydrogen provided by the ammonia molecules seems to play no role in determining the final nanostructure [35]. The other films show a less ordered nanostructure and are composed of narrowly bent graphene planes having a higher perimeter to area ratio, suggesting that nitrogen atoms are mainly located at the edge of graphene planes and bonded in pyridine-like structures (high intensity of the peak at 398.8 eV).

Supported by these observations we can easily include the role of oxygen in our description: thanks to their high porosity and effective surfaces (greater than 700 m^2/g) [36], upon exposure to atmosphere our films can adsorb a consistent amount of oxygen. Oxygen saturates the dangling bonds present in great amount in our materials and chemically reacts with unstable carbon structures (previous electron spectroscopy [37] and NEXAFS[2] experiments performed in-situ on ns-C freshly deposited films demonstrated that no oxygen contamination occurs during the deposition process). This explains why high oxygen concentrations have been measured by XPS even if oxygen is not supplied during the synthesis of the films, and why the position and shape of O 1s edge peak is the same for all materials. Therefore we conclude that oxygen does not participate in the formation of our ordered nanostructures.

4. Conclusions

We have characterized CN_x films grown by supersonic cluster beam deposition. Nitrogen can be incorporated in the nanostructured films both by supplying N during cluster formation and by assisting the cluster deposition with a N ion bombardment. Nitrogen to carbon percentage can be varied between 1% and 20%. The film nanostructure can be controlled by varying the synthesis route. In particular in NH_3 gas synthesized ns-C the nanostructure is characterized by bundles of well-ordered graphene multilayers, onions and nanotubes embedded in an amorphous matrix. This resembles the structures of films obtained by anodic jet carbon arc

[2] C. Lenardi, P. Piseri, G. Bongiorno, D. Bandiera, E. Barborini, P. Milani, L. Ravagnan, F. Siviero, E. Salis, M. Coreno, M. De Simone. Preliminary results with CESYRA (Cluster Experiments with SYnchrotron RAdiation). Unpublished.

methods [15] or unbalanced reactive magnetron sputtering [16].

Using XPS characterization we have demonstrated that N bonds to sp^2 graphite-like carbon structure substituting C atoms either in the middle of a graphite sheet or at its edge. Oxygen instead is found to saturate dangling bonds in the film upon exposure to air.

Supersonic cluster beam deposition, which can achieve extremely high deposition rates compared to other deposition technique, allows the control over N content and film nanostructure by changing the PMCS operation parameters. Thanks to the high directionality of the supersonic beam substrate patterning with stencil masks can be realized, making the deposition technique compatible with other planar microtechnologies [7]. The mechanical properties of our films are not comparable in terms of hardness and elasticity [16] with those reported by other authors since the low kinetic energy of the clusters in the supersonic beam does not favor the formation of links between the nanoparticles. SCBD may be interesting for the embedding of nanoparticles with controlled nanostructure into hard matrices to improve their mechanical properties.

Acknowledgments

We acknowledge financial support from the European Community under IHP Network: Synthesis structure and properties of new Fullerene like materials (HPRN-CT-2002-00209) and from MIUR under FIRB project Carbon Micro- and Nanostructures.

References

[1] Liu AY, Cohen ML. Prediction of new low compressibility solids. Science 1989;245:841–2.
[2] Kroto HW, Heath JR, O'Brien SCO, Curl RF, Smally RE. C_{60}: Buckminsterfullerene. Nature 1985;318:162–3.
[3] Iijima S. Helical microtubes of graphite carbon. Nature 1991;354:56–8.
[4] Neidhardt J, Hultman L, Czigány Zs. Correlated high resolution transmission electron microscopy and X-ray photoelectron spectroscopy studies of structured CN_x ($0 < x < 0.25$) thin solid films. Carbon 2004;42(12–13):2729–34.
[5] Alexandrou I, Baxendale M, Rupesinghe NL, Amaratunga GAJ, Kiely CJ. Field emission properties of nanocomposite carbon nitride films. J Vac Sci Technol B 2000;18(6):2698–703.
[6] Radnòczi G, Kovàcs GyJ, Pécz B, Geszti O, Sàfràn G. Fullerene-like structures in CN_x particles. Vacuum 2003;71(1–2):185–91.
[7] Barborini E, Piseri P, Podesta' A, Milani P. Cluster beam microfabrication of patterns of three-dimensional nanostructured objects. Appl Phys Lett 2000;77(7):1059–61.
[8] Barborini E, Piseri P, Milani P. A pulsed microplasma source of high intensity supersonic carbon cluster beams. J Phys D 1999;32(21):L105–9.
[9] Casari CS, Li Bassi A, Ravagnan L, Siviero F, Lenardi C, Piseri P, et al. Chemical and thermal stability of carbyne-like structures in cluster-assembled carbon films. Phys Rev B 2004;69(7):75422–7.
[10] Agostino RG, Caruso T, Chiarello G, Cupolillo A, Pacilè D, Filosa R, et al. Thermal annealing and hydrogen exposure effects on cluster-assembled nanostructured carbon films embedded with transition metal nanoparticles. Phys Rev B 2003;68(3): 35413–25.
[11] Liu P, Ziemann PJ, Kittelson DB, McMurry PH. Generating PARTICLE BEAMS OF CONTROLLED DIMENSIONS AND DIVERGENCE: I. Theory of particle motion in aerodynamic lenses and nozzle expansions. Aerosol Sci Technol 1995;22(3): 293–313.
[12] Liu P, Ziemann PJ, Kittelson DB, McMurry PH. Generating particle beams of controlled dimensions and divergence: II. Experimental evaluation of particle motion in aerodynamic lenses and nozzle expansions. Aerosol Sci Technol 1995;22(3): 314–24.
[13] Di Fonzo F, Gidwani A, Fan MH, Neumann D, Iordanoglou DI, Heberlein JVR, et al. Focused nanoparticle-beam deposition of patterned microstructures. Appl Phys Lett 2000;77(6):910–2.
[14] Lavin JG, Subramoney S, Ruoff RS, Berber S, Tomànek D. Scrolls and nested tubes in multiwall carbon nanotubes. Carbon 2002;40(7):1123–30.
[15] Alexandrou I, Kiely CJ, Papworth AJ, Amaratunga GAJ. Formation and subsequent inclusion of fullerene-like nanoparticles in nanocomposite carbon thin film. Carbon 2004;42 (8–9):1651–6.
[16] Neidhardt J, Czigány Zs, Brunell IF, Hultman L. Growth of fullerene-like carbon nitride thin solid films by reactive magnetron sputtering; role of low-energy ion irradiation in determining microstructure and mechanical properties. J Appl Phys 2003; 93(5):3002–15.
[17] Czigány Zs, Neidhardt J, Brunell IF, Hultman L. Imaging of fullerene-like structures in CN_x thin films by electron microscopy; sample preparation artefacts due to ion-beam milling. Ultramicroscopy 2003;94(3–4):163–73.
[18] Tsai H, Bogy DB. Critical review characterization of diamondlike carbon films and their application as overcoats on thin-film media for magnetic recording. J Vac Sci Technol A 1987;5(6):3287–312.
[19] Ajayan PM, Iijima S, Ichihashi T. Electron-energy-loss spectroscopy of carbon nanometer-size tubes. Phys Rev B 1993;47(11): 6859–62.
[20] Manour A, Ugolini D. Photoelectron-spectroscopy study of amorphous a-CN_x:H. Phys Rev B 1993;47(16):10201–9.
[21] Zaluzec NJ. An electron energy loss spectral library. Ultramicroscopy 1982;9(3):319–23.
[22] Hirai H, Terauchi M, Tanaka M, Kondo K. Estimating band gap of amorphous diamond and nanocrystalline diamond powder by electron energy loss spectroscopy. Diamond Relat Mater 1999;8(8–9):1703–6.
[23] Suenaga K, Sandré E, Colliex C, Pickard CJ, Kataura H, Iijima S. Electron energy-loss spectroscopy of electron states in isolated carbon nanostructures. Phys Rev B 2001;63(16):165404–8.
[24] Trasobares S, Stéphan O, Colliex C, Hsu WK, Kroto HW, Walton DRM. Compartmentalized CN_x nanotubes: chemistry, morphology, and growth. J Chem Phys 2002;116(20):8966–72.
[25] Han W, Kohler-Redlich P, Seeger T, Ernst F, Rühle M, Grobert N, et al. Aligned CN_x nanotubes by pyrolysis of ferrocene/C60 under NH_3 atmosphere. Appl Phys Lett 2000;77(12):1807–9.
[26] Amaratunga GAJ, Chhowalla M, Kiely CJ, Alexandrou I, Aharonov R, Devenish RM. Hard elastic carbon thin films from linking of carbon nanoparticles. Lett Nature 1996;383(26): 321–3.
[27] Sette F, Wertheim GK, Ma Y, Meigs G, Modesti S, Chen CT. Lifetime and screening of the C 1s photoemission in graphite. Phys Rev B 1990;41(14–15):9766–70.
[28] Hammer P, Lacerda RG, Droppa Jr R, Alvarez F. Comparative study on the bonding structure of hydrogenated and hydrogen free carbon nitride films with high N content. Diamond Relat Mater 2000;9(3–6):577–81.

[29] Hammer P, Victoria NM, Alvarez F. Electronic structure of hydrogenated carbon nitride films. J Vac Sci Technol A 1998;16(5):2941–9.
[30] Beamson G, Briggs D. High resolution XPS of organic polymers—The Scienta ESCA database. Chichester, UK: John Wiley & Sons Ltd.; 1992.
[31] Ronning C, Feldermann H, Merk R, Hofsäss H, Reinke P, Thiele JU. Carbon nitride deposited using energetic species: a review on XPS studies. Phys Rev B 1998;58(4):2207–15.
[32] Lee WH, Lee JG, Reucroft PJ. XPS study of carbon fiber surfaces treated by thermal oxidation in a gas mixture of $O_2/(O_2 + N_2)$. Appl Surf Sci 2001;171(1–2):136–42.
[33] Lopez S, Dunlop HM, Benmalek M, Tourillon G, Wong MS, Sproul WD. XPS, XANES and ToF-SIMS characterization of reactively magnetron-sputtered carbon nitride films. Surf Int Anal 1997;25(5):315–23.
[34] Hellgren N, Johansson MP, Broitman E, Hultman L, Sundgren JE. Role of nitrogen in the formation of hard and elastic CN_x thin films by reactive magnetron sputtering. Phys Rev B 1999;59(7):5162–9.
[35] Silva SRP, Robertson J, Amaratunga GAJ, Rafferty B, Brown LM, Schwan J, Franceschini DF, et al. Nitrogen modification of hydrogenated amorphous carbon films. J Appl Phys 1997;81(6):2626–34.
[36] Lenardi C, Barborini E, Briois V, Lucarelli L, Piseri P, Milani P. NEXAFS characterization of nanostructured carbon thin films exposed to hydrogen. Diamond Relat Mater 2001;10:863–8.
[37] Magnano E, Cepek C, Sancrotti M, Siviero F, Vinati S, Lenardi C, et al. In situ growth and thermal treatment of nanostructured carbon produced by supersonic cluster beam deposition: an electron spectroscopy investigation. Phys Rev B 2003;67(12):125414–7.